SEMARAK ILMU PUBLISHING

Journal of Advance Research in Applied Sciences and Engineering Technology

Journal homepage:
https://semarakilmu.com.my/journals/
ISSN: XXXX-XXXX

Electrochemical Performance of S-rGO Electrodes on Different Aqueous Electrolytes of Supercapacitor Applications

Nurul Hazwani Aminuddin Rosli[1,*], Intan Juliana Shamsudin[2], Azuraida Amat[1], Nor Azlian Abdul Manaf[1], Nurazlin Ahmad[1], Azima Azmi[3], Chin Hua Chia[4]

[1] Physics Department, Centre for Defence Foundation Studies, Universiti Pertahanan Nasional Malaysia, 57000 Kuala Lumpur, Malaysia
[2] Chemistry & Biology Department, Centre for Defence Foundation Studies, National Defence University of Malaysia, Kem Sungai Besi, Kuala Lumpur 57000, Malaysia
[3] Biotechnology & Nanotechnology Research Centre, MARDI Headquarters, Persiaran MARDI-UPM, 43400 Serdang, Selangor, Malaysia
[4] Materials Science Program, Faculty of Science and Technology, Universiti Kebangsaan Malaysia, 43600 Bangi, Selangor, Malaysia

ARTICLE INFO

Article history:
Received 29 October XXXX
Received in revised form 1 December XXXX
Accepted 9 December XXXX
Available online 10 December XXXX

Keywords:

Graphene; Heteroatoms; Energy Storage

ABSTRACT

Improvement in the supercapacitive performance of heteroatom-doped graphene may only be obtained by heteroatom redox behavior. We investigated sulfur doped reduced graphene oxide (S-rGO) synthesis utilising microwave reactor assisted processes using sodium sulfide hydrate (Na_2S) as sulfur precursors. An experimental investigation was conducted to comprehend the electrochemical behaviour in various aqueous electrolytes for instance sulfuric acid (H_2SO_4), potassium sulfate (K_2SO_4), and potassium hydroxide (KOH). Various methods were employed to evaluate the electrochemical performing of the S-rGO electrode, for example cyclic voltammetry (CV), galvanostatic charge-discharge (GCD), and electrical impedance spectroscopy (EIS). S-rGO electrode in 1 M H_2SO_4 exhibit the superior specific capacitance (C_{sp}) up to 352 Fg^{-1} at 0.5 Ag^{-1}.

1. Introduction

Aside from the limiting environmental resources derived from fossil fuel energy and ecological-climate challenges. The use of energy from renewable sources is now recognized as one of the most proposed worldwide approaches to growing electric power and energy demand. Supercapacitors (SCs), a form of device that stores electricity between secondary batteries and typical capacitors, have generated a lot of interest owing to their enormous high-power capability and extended cycle stability when compared to batteries [1]. The advantages of SCs are large power density, an elevated charging rate, efficient charging and discharging speeds, excellent charging and discharging rates, and greater cycle durability [2,3].

In general, supercapacitors are often classified into two kinds such as pseudocapacitors (PCs) and electrochemical double-layer capacitors (EDLCs). PCs store charge by a fast faradic redox process composed of metal sulfides, metal oxides, and polymers that have an excellent specific capacitance (C_{sp}) but low cycle stability. But materials for EDLC, like graphene, carbon nanotubes

* *Corresponding author.*
E-mail address: n.hazwani@upnm.edu.my

(CNT), and activated carbon (AC) which store energy by separating charge at electrode/electrode contacts offer great cycling stability but weak C_{sp} [4]. Industrial supercapacitors are presently driven by EDLCs made of carbon-based substances because of their enormous surface area, simplicity of modification, and higher mobility. As a result, significant efforts have been put towards overcoming prior challenges by developing SCs using both EDLC and PCs materials. The integration of EDLC with PCs may not only increase the C_{sp} but also boost the long-cycle stability [5]. The use of heteroatoms for instance boron (B), phosphorus (P), nitrogen (N), and sulfur (S) with carbon materials is a major method for increasing energy density [6,7]. Incorporating heteroatoms into carbon materials could be a successful method to improve the capacity of carbon materials via pseudocapacitive impact resulting through faradic behaviours associated with the presence of heteroatom species, along with boosting the wetting ability for carbon substances in an aqueous electrolyte [8,9]. Graphene represents a viable contender for enhanced electrode materials because of its large specific area of surface, rapid intrinsic transport flexibility, as well as outstanding physical characteristics [10].

Electrolytes have a stronger influence on defining the efficiency of supercapacitors and play a key part in the efficiency of the device [11]. EDLCs employ two types of electrolytes: aqueous and organic electrolytes; aqueous electrolytes are more suited than organic electrolytes because of their cost-effectiveness, favourable conductance, minimum resistance inside, and non-flammability [12]. This is due to an immediate connection between the SC's energy density and its voltage of operation [13]. Typically, types of electrolytes that are been used, such as sulfuric acid (H_2SO_4), sodium sulfate (Na_2SO_4), potassium sulfate (K_2SO_4), potassium hydroxide (KOH), and sodium hydroxide (NaOH) [14–16]. They have different hydrated radius (H^+ = 2.80 Å, K^+ = 3.31 Å) and molar ionic conductivity (H^+ = 35 mSm^2mol^{-1}, K^+ = 7.35 mSm^2mol^{-1}) of each ion in the electrolytes [17].

To our knowledge, there has been no research available on the study comparison of impacts of electrochemical efficiency of sulfur-doped reduced graphene oxide (S-rGO) electrode for different aqueous electrolytes (acid, alkaline, and neutral). This research examines three different aqueous electrolytes for SCs application using the method of cyclic voltammetry (CV), galvanostatic charge-discharge (GCD) evaluation, and electrical impedance spectroscopy (EIS).

2. Methodology

2.1 Materials

Potassium permanganate ($KMnO_4$, >99%), sulfuric acid (H_2SO_4, 95–97%), and hydrogen peroxide (H_2O_2, 30%) purchased from Merck Millipore. Phosphoric acid (H_3PO_4, 85%) and hydrochloric acid (HCl, 37%) from R&M Chemicals. Sodium sulfide hydrate (Na_2S, ≥60%), poly(vinylidene fluoride) (PVdF, Mw ~534,000), graphite flakes (+100 mesh, ≥75% min), and potassium hydroxide (KOH, ≥85) from Sigma Aldrich. Carbon cloth from Ce-tech Co., Ltd. 1-methyl-2-pyrrolidinone (NMP, ≥99%) from Alfa Aesar. All chemicals were utilised as supplied, with no additional purification.

2.2 Sample Preparation

Graphene oxide (GO) was produced using a modified Hummer's technique [18], the specifics of GO production discussed in [19]. 5 ml of GO (0.1 wt%) and 5 ml of Na_2S with a concentration of 0.25 M will be moved into a vial and then undergo microwave-assisted production at 100 °C used for 5 minutes by microwave reactor (Monowave 300, Anton Paar). Following microwave-assisted production, the products were centrifuged at 12,000 rpm over 15 minutes. The collected substance was taken out and freeze-dried over one day. This method will produce sulfur-doped reduced

graphene oxide (S-rGO). The samples of electrode were evaluated using different aqueous electrolytes acid (H_2SO_4), alkaline (KOH), and neutral (K_2SO_4) were respectively denoted as S-rGO (H_2SO_4), S-rGO (KOH), and S-rGO (K_2SO_4).

2.3 Electrochemical Analysis

The electrical behaviour S-rGO electrodes were evaluated through a three-electrode setup with 1 M H_2SO_4, 1 M KOH and 1 M K_2SO_4 serving as electrolytes. Electrochemical performance of S-rGO electrodes were investigated via CV, GCD, and EIS and conducted by Reference 600, Gamry potentiostat. Platinum wire for the counter electrode, Ag/AgCl electrode point as reference electrode will be used. Working electrode, S-rGO samples were pasted on the carbon cloth. The C_{sp} for the electrodes was calculated by Eq. (1) presented below [20].

$$C_{sp} = \frac{I \times t}{m \times \Delta V} \tag{1}$$

where I = charging current, t = discharge time, m = mass loading, and ΔV = discharging potential window, respectively. EIS was used to analyse the samples' fundamental behaviour.

3. Results

3.1 Cyclic Voltammetry Analysis

CVs are used to assess the electrochemical characteristics of supercapacitors in various electrolytes. Figure 1 (a) shows the CV of S-rGO electrodes with different electrolytes (1 M H_2SO_4, 1 M KOH, and 1 M K_2SO_4) with a scan rate of 50 mVs^{-1}. The CV curves observed for S-rGO electrodes displayed quasi-rectangular cycles owing to the dominance of EDLC features, demonstrating outstanding electrical double-layer capacitance behaviour [21]. The potential range of CV curves for S-rGO (H_2SO_4), S-rGO (KOH), and S-rGO (K_2SO_4) electrodes was between 0 – 0.8 V, -0.8 – 0 V, and -0.8 – 0.8 V, respectively. These differences in potential ranges depend on the characteristics of electrolytes [11]. From Figure 1, S-rGO (K_2SO_4) electrodes have a larger curve compared to the other electrodes. This is owing to the nature of the K_2SO_4 electrolyte, which is neutral [17], Because of a shortage of H^+ ions, the overpotential for H_2 creation is considerable, which might have moved the hydrogen evolution reaction (HER) to a more lower negative potential [22]. Also, S-rGO (K_2SO_4) electrode has the highest current response at 0.8 V. The discrepancies found within the current sensitivity and CV behaviours of S-rGO electrodes in different electrolytes are due to the physical features possessed by the ions present in electrolytes. These features comprise ionic radius, ionic hydration radius, molar electrical conductivity, and ion mobility [13]. Meanwhile, S-rGO (H_2SO_4) electrode has a relatively high concentration of H^+ ions. While S-rGO (KOH) electrode displays the smallest curve compared to the other electrodes due to the presence (OH^-) in the basic medium which induced the oxygen evolution reaction (OER) [22]. Fig. 1 (b) – (d) reveals CV performance of various electrolytes by the scan rate of 10 – 200 mV s^{-1}. When the scan rate rises, the results resemble quasi-rectangular curves.

3.2 Galvanostatic Charge-Discharge

GCD testing was achieved to assess S-rGO electrodes materials rate performance. Figure 2 (a) and (b) shows GCD curves at 0.5 Fg^{-1} for H_2SO_4, KOH, and K_2SO_4 electrolytes, respectively. GCD curves

offer the key properties of supercapacitor behaviour, including specific capacitance. The S-rGO curves for three electrodes in different electrolytes show a near to triangular shape, demonstrating an optimal capacitive performance and a balance charge across electrodes, suggesting EDLC behaviour is caused by irreversible interactions between electrodes along with electrolytes [23,24]. It has been observed when the potential decline was found at the beginning of discharge, it could be attributable towards the internal resistance within the material of the electrode. This could be related to its characteristics such as electrode-electrolyte resistance during contact, electrolyte solution resistance, as well as charge transfer barrier. As current density increases, so does the electrode material's internal resistance [25]. Figure 2 (c) points out the correlation involving discharge time with current density, which decreases when current density increases. These demonstrate the influence of a potential shift upon electrochemical motion because charges become slow in getting deeper through the surface of an electrode [26]. S-rGO (H_2SO_4) electrode revealed the highest C_{sp} 352 Fg^{-1} by scan rate 0.5 Ag^{-1}, compared to C_{sp} of S-rGO (KOH) and S-rGO (K_2SO_4) that display 99 and 119 Fg^{-1}. Clearly, from Figure 3, the C_{sp} dropped with increased density of current, because the ions had insufficient time for diffusion through each pore at a rapid pace [27]. The variation C_{sp} is due to the ionic radius of hydrated, ionic movements, as well as molar ionic conductivity, while H_2SO_4 has a smaller cationic radius, greater ionic movements, and greater molar conductivity [28].

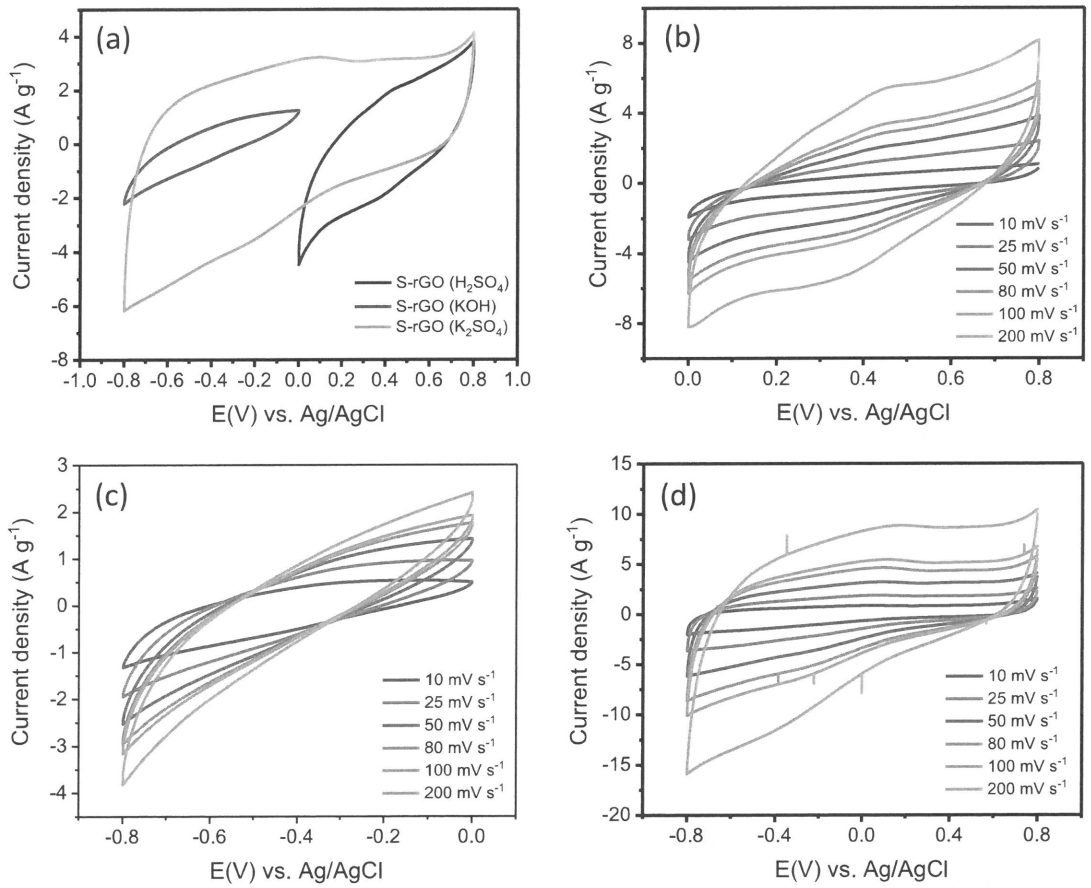

Fig. 1 (a) CV curves at scan rates of 50 mVs^{-1}, CV curves for different scan rates in (b) H_2SO_4 electrolyte, (c) KOH electrolyte, and (d) K_2SO_4 electrolyte.

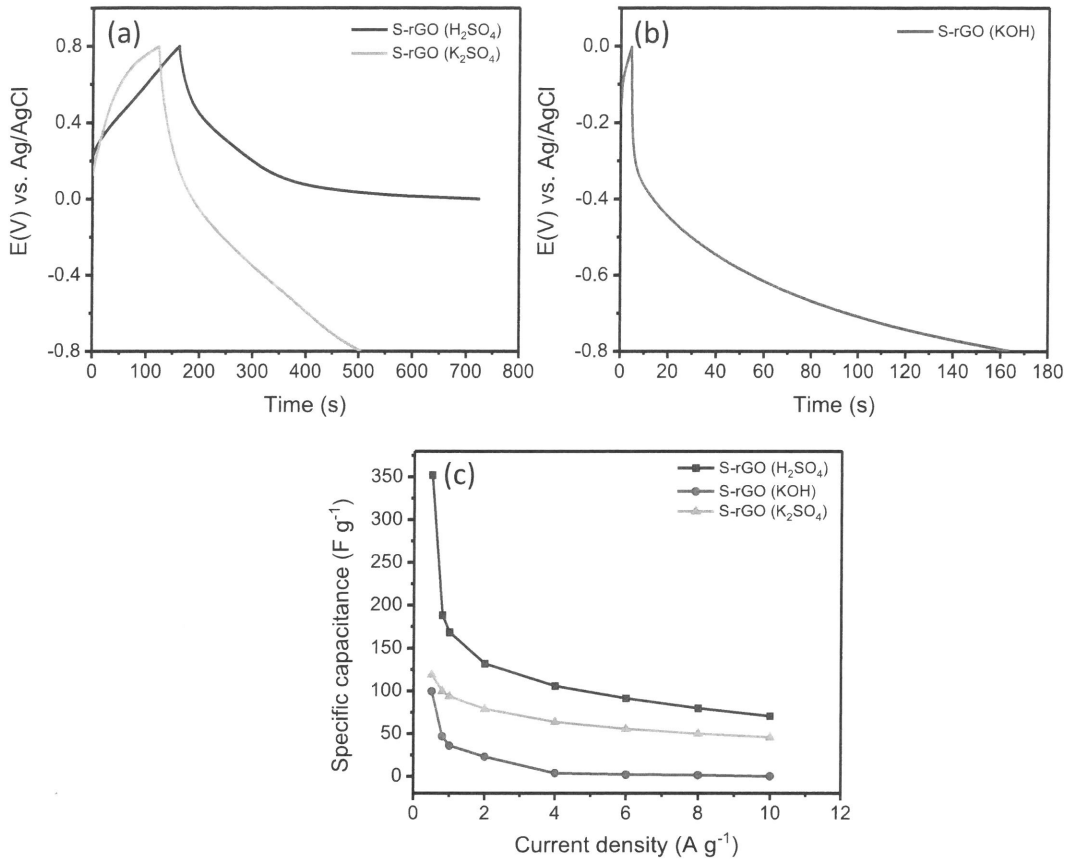

Fig. 2 GCD graphs of (a) S-rGO electrodes in H_2SO_4 and K_2SO_4 electrolytes and (b) S-rGO electrode in KOH electrolyte. (c) Specific capacitance versus current density of S-rGO electrode in different electrolytes.

3.3 *Electrochemical Impedance Spectroscopy*

EIS was tested for S-rGO electrodes in different electrolytes to investigate the restrictions of ions of electrode substances. Figure 4 shows a Nyquist plot of S-rGO electrodes. For high-frequency regions, the point of intersection created along the horizontal line of a Nyquist plot shows the internal resistance (R_s). One depressed semicircle was seen in the high-to-medium frequency area, which is connected to the outermost feature on the electrodes, correlating to the resistance to charge transfer (R_{ct}) across the interface of the electrode with electrolyte. Whereas, a spike existed discovered in the low-frequency band, suggesting a good edge nature involving electrolyte with electrode [29]. As a result of Figure 3, the R_s values for different electrolytes are about 0.1, 1.6, and 3.3 Ω for supercapacitors in H_2SO_4, KOH, and K_2SO_4, respectively. S-rGO (H_2SO_4) electrode obtained the smallest value because of the tiny transfer path of ions [30]. Meanwhile, R_{ct1} values obtained for S-rGO (H_2SO_4), S-rGO (KOH), and S-rGO (K_2SO_4) electrodes were 2.56, 144.8, and 28.2 Ω, whereas R_{ct2} were 1.8, 30.3, and 2.6 Ω. Higher values observed for S-rGO (KOH) electrode are ascribed to the poor conductivity of the material. S-rGO (H_2SO_4) electrode had the lowest R_{ct} value of any of the tested electrodes, suggesting that it has the quickest transfer of charge and diffusion of ions on the surface of the electrode contact; this is due to its greater C_{sp}. Low R_{ct} values contribute to the performance of the supercapacitor by allowing it to store and distribute energy efficiently.

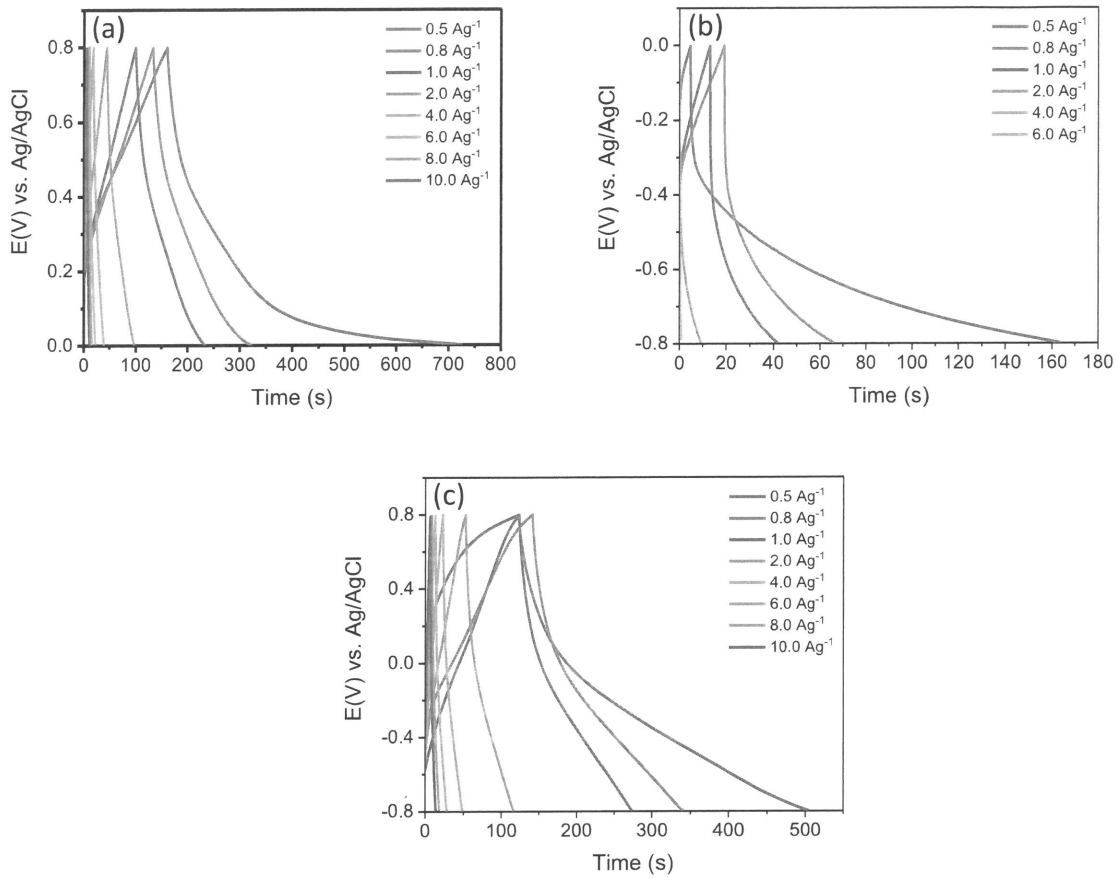

Fig. 3 GCD graphs of S-rGO electrodes at different current densities in (a) H_2SO_4 electrolyte, (b) KOH electrolyte, and (c) K_2SO_4 electrolyte.

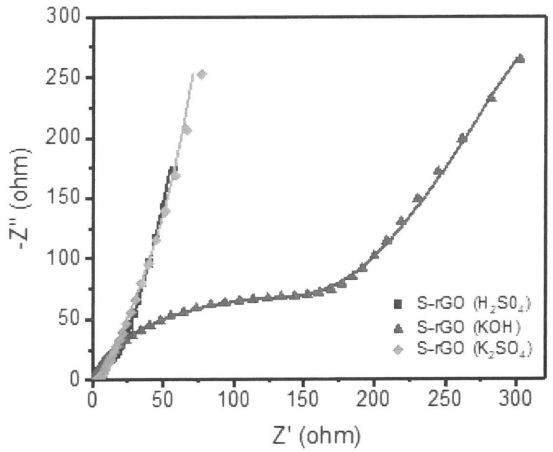

Fig. 4 Nyquist plots for S-rGO electrodes for different electrolytes.

4. Conclusions

To summarise, by evaluating the electrochemical capabilities of S-rGO electrodes utilising CV, GCD, and EIS with various electrolytes such as 1 M H_2SO_4, 1 M KOH, and 1 M K_2SO_4. S-rGO in H_2SO_4 displays the highest C_{sp} up to 352 Fg^{-1} compared to S-rGO in KOH (99 Fg^{-1}) and K_2SO_4 (119 Fg^{-1}), respectively. The smallest R_s and R_{ct} are obtained by S-rGO electrode in H_2SO_4. This is due to the properties of electrolytes for example ionic radius, ionic hydration radius, molar electrical conductivity, and ion mobility. This study introduces a new approach to producing S-rGO electrode and their efficient use in energy storage.

Acknowledgement
The authors thankfully acknowledge the financial support from the Centre for Research and Innovation Management, UPNM, for funding this research through the grant scheme (Code Grant: UPNM/2023/GPJP/STG/6).

References

[1] Chen, C., Zhang, Q., Ma, T., and Fan, W., "Synthesis and Electrochemical Properties of Nitrogen-Doped Graphene/Copper Sulphide Nanocomposite for Supercapacitor," *Journal of Nanoscience and Nanotechnology*, Vol. 17, No. 4, 2017, pp. 2811–2816. https://doi.org/10.1166/jnn.2017.12668

[2] Tang, H., Yao, J., and Zhu, Y., "Recent Developments and Future Prospects for Zinc-Ion Hybrid Capacitors: A Review," *Advanced Energy Materials*, Vol. 11, No. 14, 2021, pp. 2003994–2004016. https://doi.org/10.1002/aenm.202003994

[3] Yadlapalli, R. T., Alla, R. K. R., Kandipati, R., and Kotapati, A., "Super Capacitors for Energy Storage: Progress, Applications and Challenges," *Journal of Energy Storage*, Vol. 49, 2022, pp. 104194–1041204. https://doi.org/10.1016/j.est.2022.104194

[4] Suriyakumar, S., Bhardwaj, P., Grace, A. N., and Stephan, A. M., "Role of Polymers in Enhancing the Performance of Electrochemical Supercapacitors: A Review," *Batteries and Supercaps*, Vol. 4, No. 4, 2021, pp. 571–584. https://doi.org/10.1002/batt.202000272

[5] Ji, Y., Deng, Y., Wu, H., and Tong, Z., "In Situ Preparation of P, O Co-Doped Carbon Spheres for High-Energy Density Supercapacitor," *Journal of Applied Electrochemistry*, Vol. 49, No. 6, 2019, pp. 599–607. https://doi.org/10.1007/s10800-019-01308-z

[6] Kiran, S. K., Shukla, S., Struck, A., and Saxena, S., "Surface Enhanced 3D RGO Hybrids and Porous RGO Nano-Networks as High Performance Supercapacitor Electrodes for Integrated Energy Storage Devices," *Carbon*, Vol. 158, 2020, pp. 527–535. https://doi.org/10.1016/j.carbon.2019.11.021

[7] Wang, M., Yang, J., Liu, S., Li, M., Hu, C., and Qiu, J., "Nitrogen-Doped Hierarchically Porous Carbon Nanosheets Derived from Polymer/Graphene Oxide Hydrogels for High-Performance Supercapacitors," *Journal of Colloid and Interface Science*, Vol. 560, 2020, pp. 69–76. https://doi.org/10.1016/j.jcis.2019.10.037

[8] Talebi, M., Asen, P., Shahrokhian, S., and Ahadian, M. M., "Polyphosphate-Reduced Graphene Oxide on Ni Foam as a Binder Free Electrode for Fabrication of High Performance Supercapacitor," Elsevier Ltd, 2019. https://doi.org/10.1016/j.electacta.2018.10.192

[9] Hu, F., Zhang, T., Wang, J., Li, S., Liu, C., Song, C., Shao, W., Liu, S., and Jian, X., "Constructing N, O-Containing Micro/Mesoporous Covalent Triazine-Based Frameworks toward a Detailed Analysis of the Combined Effect of N, O Heteroatoms on Electrochemical Performance," *Nano Energy*, Vol. 74, 2020, pp. 104789–104798.

https://doi.org/10.1016/j.nanoen.2020.104789

[10] Ahmad, F., Zahid, M., Jamil, H., Khan, M. A., Atiq, S., Bibi, M., Shahbaz, K., Adnan, M., Danish, M., Rasheed, F., Tahseen, H., Shabbir, M. J., Bilal, M., and Samreen, A., "Advances in Graphene-Based Electrode Materials for High-Performance Supercapacitors: A Review," *Journal of Energy Storage*, Vol. 72, 2023, pp. 108731–108747. https://doi.org/10.1016/j.est.2023.108731

[11] Mendhe, A., and Panda, H. S., "A Review on Electrolytes for Supercapacitor Device," *Discover Materials*, Vol. 3, No. 1, 2023, pp. 29–55. https://doi.org/10.1007/s43939-023-00065-3

[12] Verma, R., Didwal, P. N., Hwang, J. Y., and Park, C. J., "Recent Progress in Electrolyte Development and Design Strategies for Next-Generation Potassium-Ion Batteries," *Batteries and Supercaps*, Vol. 4, No. 9, 2021, pp. 1428–1450. https://doi.org/10.1002/batt.202100029

[13] Barzegar, F., Momodu, D. Y., Fashedemi, O. O., Bello, A., Dangbegnon, J. K., and Manyala, N., "Investigation of Different Aqueous Electrolytes on the Electrochemical Performance of Activated Carbon-Based Supercapacitors," *RSC Advances*, Vol. 5, No. 130, 2015, pp. 107482–107487. https://doi.org/10.1039/c5ra21962k

[14] Periasamy, P., Krishnakumar, T., Sandhiya, M., Sathish, M., Chavali, M., Siril, P. F., and Devarajan, V. P., "Preparation and Comparison of Hybridized WO_3–V_2O_5 Nanocomposites Electrochemical Supercapacitor Performance in KOH and H_2SO_4 Electrolyte," *Materials Letters*, Vol. 236, 2019, pp. 702–705. https://doi.org/10.1016/j.matlet.2018.11.050

[15] Wu, H., Wang, X., Jiang, L., Wu, C., Zhao, Q., Liu, X., Hu, B., and Yi, L., "The Effects of Electrolyte on the Supercapacitive Performance of Activated Calcium Carbide-Derived Carbon," *Journal of Power Sources*, Vol. 226, 2013, pp. 202–209. https://doi.org/10.1016/j.jpowsour.2012.11.014

[16] Venkateshalu, S., Goban Kumar, P., Kollu, P., Jeong, S. K., and Grace, A. N., "Solvothermal Synthesis and Electrochemical Properties of Phase Pure Pyrite FeS_2 for Supercapacitor Applications," *Electrochimica Acta*, Vol. 290, 2018, pp. 378–389. https://doi.org/10.1016/j.electacta.2018.09.027

[17] Ibukun, O., and Jeong, H. K., "Effects of Aqueous Electrolytes in Supercapacitors," *New Physics: Sae Mulli*, Vol. 69, No. 2, 2019, pp. 154–158. https://doi.org/10.3938/NPSM.69.154

[18] Huang, N. M., Lim, H. N., Chia, C. H., Yarmo, M. A., and Muhamad, M. R., "Simple Room-Temperature Preparation of High-Yield Large-Area Graphene Oxide," *International journal of nanomedicine*, Vol. 6, 2011, pp. 3443–3448. https://doi.org/10.2147/ijn.s26812

[19] Rosli, N. H. A., Lau, K. S., Winie, T., Chin, S. X., and Chia, C. H., "Synergistic Effect of Sulfur-Doped Reduced Graphene Oxide Created via Microwave-Assisted Synthesis for Supercapacitor Applications," *Diamond and Related Materials*, Vol. 120, 2021, pp. 108696–108705. https://doi.org/10.1016/j.diamond.2021.108696

[20] Guo, G., Shen, L., Li, X., Cao, Y., Sun, Y., and Xiong, Z., "Tunable Reduction Degree of Stacked Lamellar RGO Film for Application in Flexible All-Solid-State Supercapacitors," *Diamond and Related Materials*, Vol. 106, No. April, 2020, p. 107845. https://doi.org/10.1016/j.diamond.2020.107845

[21] Wang, Q., Plylahan, N., Shelke, M. V., Devarapalli, R. R., Li, M., Subramanian, P., Djenizian, T., Boukherroub, R., and Szunerits, S., "Nanodiamond Particles/Reduced Graphene Oxide Composites as Efficient Supercapacitor Electrodes," *Carbon*, Vol. 68, 2014, pp. 175–184. https://doi.org/10.1016/j.carbon.2013.10.077

[22] Thareja, S., and Kumar, A., "High Electrochemical Performance of 2.5 V Aqueous Symmetric Supercapacitor Based on Nitrogen-Doped Reduced Graphene Oxide," *Energy Technology*. 5. Volume 8, 1901339–1901349. https://doi.org/10.1002/ente.201901339

[23] Chen, Q., Li, X., Zang, X., Cao, Y., He, Y., Li, P., Wang, K., Wei, J., Wu, D., and Zhu, H., "Effect of Different Gel Electrolytes on Graphene-Based Solid-State Supercapacitors," *RSC Advances*, Vol. 4, No. 68, 2014, pp. 36253–36256. https://doi.org/10.1039/c4ra05553e

[24] Kim, T., Subedi, S., Dahal, B., Chhetri, K., Mukhiya, T., Muthurasu, A., Gautam, J., Lohani, P. C., Acharya, D., Pathak, I., Chae, S.-H., Ko, T. H., and Kim, H. Y., "Homogeneous Elongation of N-Doped CNTs over Nano-Fibrillated Hollow-Carbon-Nanofiber Mass," *Advanced S*, Vol. 9, 2022, pp. 2200650–2200660. https://doi.org/DOI: 10.1002/advs.202200650

[25] Sankar, K. V., Kalpana, D., and Selvan, R. K., "Electrochemical Properties of Microwave-Assisted Reflux-Synthesized Mn_3O_4 Nanoparticles in Different Electrolytes for Supercapacitor Applications," *Journal of Applied Electrochemistry*, Vol. 42, No. 7, 2012, pp. 463–470. https://doi.org/10.1007/s10800-012-0424-2

[26] Ma, T., Ni, Y., Wang, Q., Xiao, J., Huang, Z., Tao, Z., and Chen, J., "Lithium Dendrites Inhibition by Regulating Electrodeposition Kinetics," *Energy Storage Materials*, Vol. 52, 2022, pp. 69–75. https://doi.org/10.1016/j.ensm.2022.07.038

[27] Xu, D., Wan, M., Yang, Y., Pan, B., and Chen, Q., "Mesopore-Dominated Porous Carbon Derived from Vinasse for High Performance Supercapacitors with Different Electrolytes," *Industrial Crops and Products*, Vol. 187, 2022, pp. 115462–115472. https://doi.org/10.1016/j.indcrop.2022.115462

[28] Awitdrus, Suwandi, D. A., Agustino, Taer, E., Farma, R., and Syahputra, R. F., "Effect of Aqueous Electrolyte to the Supercapacitor Electrode Performance Made from Sugar Palm Fronds Waste," *Journal of Physics: Conference Series*, Vol. 1951, No. 1, 2021, pp. 12009–12017. https://doi.org/10.1088/1742-6596/1951/1/012009

[29] Cheng, J., Lu, Z., Zhao, X., Chen, X., and Liu, Y., "Green Needle Coke-Derived Porous Carbon for High-Performance Symmetric Supercapacitor," *Journal of Power Sources*, Vol. 494, 2021, pp. 229770–229779. https://doi.org/10.1016/j.jpowsour.2021.229770

[30] Wang, H., Tran, D., Moussa, M., Stanley, N., Tung, T. T., Yu, L., Yap, P. L., Ding, F., Qian, J., and Losic, D., "Improved Preparation of MoS_2/Graphene Composites and Their Inks for Supercapacitors Applications," *Materials Science and Engineering B: Solid-State Materials for Advanced Technology*, Vol. 262, No. November 2019, 2020. https://doi.org/10.1016/j.mseb.2020.114700